Novel Clinical Anatomic Emergences and Distribution of the Facial Branches of the Ophthalmic Artery

Li-Yao Cong, D.D.S

Department of Dentistry

The Graduate School, Yonsei University

Novel Clinical Anatomic Emergences and Distribution of the Facial Branches of the Ophthalmic Artery

Directed by Professor Hee-Jin Kim, D.D.S., Ph.D.

The Doctoral Dissertation
submitted to the Department of Dentistry,
and the Graduate School of Yonsei University
in partial fulfillment of the requirements
for the degree of Doctoral of Dentistry

Li-Yao Cong

December 2017

This certifies that the Doctoral dissertation of Li-Yao Cong is approved.

Thesis Supervisor : **Prof. Hee-Jin Kim**

Thesis Committee Member : **Prof. Kyung-Seok Hu**

Thesis Committee Member : **Prof. Young-Chun Gil**

Thesis Committee Member : **Prof. Han-Sung Jung**

Thesis Committee Member : **Prof. Hun-Mu Yang**

The Graduate School
Yonsei University

December 2017

ACKNOWLEDGEMENTS

I would like to extend my heartfelt thanks to a host of people, without whose assistance the accomplishment of this thesis would have been impossible. First and foremost, I wish to express my deepest gratitude to my supervisor, Prof. Heejin Kim, who has given me the most valuable suggestions and advice during the writing of this thesis as well as in the course of my undergraduate studies. Also, Prof. Kim gave me lots of encouragement during my life in Korea. Then I am greatly indebted to Prof. Kyung-Seok Hu, who supported me very much and took care of me. I am also grateful to Prof . Young-Chun Gil, who helped me in various aspects and gave me enlightening instructions. I would also thank to Prof. Han-Sung Jung, who gave me consideration for the thesis. And Prof. Hun-Mu Yang, who gave me academic advices.

Thanks Prof. Kwan-Hyun Youn and Hyeon-Ju Kim for the fantastic figure illustration. Thanks Min-Kyu Kang for the beautiful histologic image.

I am grateful to all the assistance teachers in our anatomy lab: Hyung-Jin Lee, You-Jin Choi, Kang-Woo Lee, Kyu-Lim Lee, all of them are like my brothers and sisters. They took good care of me and helped me whenever I met difficulties both in research and in my

Korean life.

Last but not least, I am much indebted to my family, without their love and affection, I would not have enjoyed the meaningful life in the world. Also, thanks to the Prof. GuangChun Jin, who provided me this important chance for going board.

Thank you so much.

November, 2017

Author Liyao Cong

TABLE OF CONTENTS

LIST OF FIGURES

LIST OF TABLES

Abstract

Novel clinical anatomic emergences and distribution of the facial branches of the ophthalmic artery

Li-Yao Cong, D.D.S.

Department of Dentistry, The Graduate School,
Yonsei University

(Directed by Professor Hee-Jin Kim D.D.S., Ph. D.)

One of the main trunks of the ophthalmic artery (OA) exits anteriorly and emerges at the orbital region forming quite a huge arterial network to supply the forehead (supratrochlear artery, STA), the nose (dorsal nasal artery), the medial canthal region (angular artery, AA), and the eyelids (superior and inferior medial palpebral artery, SMPA and IMPA). Thus, in this study, those mentioned arterial emergences and distributions were determined as facial branches of the OA (Fbrs of OA).

Filler injectable procedures are prevalent in clinical trials for facial rejuvenation. However, dearth of well acknowledgment of Fbrs of OA, clinicians may threaten the arteries during the filler injection interventions. As a result, it may lead to skin necrosis or rare but severe blindness.

The upper eyelid myocutaneous flap (UEMF) has been used as oculoplastic surgical techniques for periorbital tissue defect reconstruction. The UEMF including the emerging point of the OA (EMP of OA) and its branches ensure

a maximal blood supply which is closely linked to the success of flap surgeries.

Therefore, the aims of this study were (1) to determine the three-dimensional (3D) location of the EMP of OA, (2) to establish a detailed topography of the forehead vascular distribution patterns of the STA and the supraorbital artery (SOA), and (3) to perform a topographic analysis of the IMPA, thereby providing the clinical guidelines for safe performances during periorbital minimally-invasive and surgical procedures.

17 hemifaces were scanned from the frontal and bilateral oblique aspects by 3D scanner (Morpheus3D®, Morpheus Company, Seongnam, Korea). The scanned face was reconstructed using Morpheus Plastic Solution (version 3.0) software. The 3D scanned images from the frontal and bilateral oblique aspects of the face were combined and merged through geometry analysis of the nearby areas at three points (lateral canthus, alare and cheilion) bilaterally. Then, the dissections on the left side of the specimen face slightly deviating right of the midline were performed. After exposure of the EMP of OA, the specimen was scanned again. Finally, the first undissected image and second half dissected image including the EMP of OA were superimposed. The EMPs of OA of 30 healthy Korean volunteers were detected by ultrasound device. Twenty hemifaces were dissected to map the arterial system of the forehead. IMPAs were examined in 31 hemifaces.

The three-dimensional location of the EMP of OA was determined. From the medial canthus to the EMP of OA, the transverse distance was 3.8±1.0 mm medially while the vertical distance was 14.0±2.9 mm superiorly. The depth from the skin to the EMP of OA was 4.8±1.7 mm by 3D scanning and was 4.5±1.1 mm by ultrasound imaging system, respectively.

Two main arterial distribution patterns of the forehead were observed based on the presence of the deep branch of the STA (dSTA). The type I

(dSTA-present pattern, 55%) was classified into two subtypes: Type Ia (35%), the layer superficial to the frontalis was supplied medially by the superficial branch of the STA (sSTA) and laterally by the superficial branch of the SOA (sSOA); the dSTA and the deep branch of the SOA (dSOA) were distributed deep to the frontalis. Type Ib (20%), the layer superficial to the frontalis was supplied by the sSTA and the sSOA in addition to the central artery or the paracentral artery; the dSTA and dSOA supplied the layer deep to the frontalis. For the type II (dSTA-absent pattern, 45%), the layer superficial to the frontalis was supplied medially by the sSTA and laterally by the sSOA; only the dSOA supplied the layer deep to the frontalis.

Four distribution patterns were observed about the IMPA. Type I (36.7%), the IMPA and SMPA branched individually from the OA, with the OA terminating as the STA on the forehead. Type II (36.7%), a short trunk branched from the OA and divided into the IMPA and SMPA, and the OA terminated as the STA. Type III (23.3%), the IMPA and SMPA arose together from the OA, and the OA terminated as the STA. Type IV (3.3%), the IMPA and SMPA were the terminal branches of the OA, with the STA arising from the AA.

Importantly, based on these results, clinicians will contribute to improve the safe outcomes when assessing the applications in the field of clinical interventions such as various dermal filler injections and UEMFs.

Key words: emergences of ophthalmic artery, supratrochlear artery, supraorbital artery, inferior medial palpebral artery, filler augmentation, 3D scanning system, ultrasound imaging system

Novel Clinical Anatomic Emergences and Distribution of the Facial Branches of the Ophthalmic Artery

Li-Yao Cong, D.D.S.

Department of Dentistry, The Graduate School,
Yonsei University

(Directed by Professor Hee-Jin Kim D.D.S., Ph.D.)

Ⅰ. INTRODUCTION

The ophthalmic artery (OA) is the first branch of the internal carotid artery distal to the cavernous sinus (Standring, 2008; Seyhan, 2013; Faris et al., 2015; Fukuta et al., 1994; Skaria, 2015; Woo et al., 2013; Yoshioka and Rhoton, 2005). There are many branches supplying the eyeball, optic nerve, and surrounding muscles. One of the main trunks of the OA, in particular, exits anteriorly and emerges at the orbital region by piercing the orbital septum inferior to the medial part of the superior orbital rim (SOR). After the emergence of the OA, the OA trunk divides into several branches, forming quite a huge arterial network to supply the upper and midface. It supplies the forehead (supratrochlear artery, STA), the nose (dorsal nasal artery, DNA), the medial

canthal region (angular artery, AA) (Fig. 1), and the eyelids (superior and inferior medial palpebral artery, SMPA and IMPA). (Cong et al., 2016; Cong et al., 2017; Kim et al., 2014; Tansatit et al., 2017; Wu et al., 2017). In this study, those arteries distributing the face were determined as facial branches of the OA (Fbrs of OA).

Dermal fillers are a popular choice among patients who wish to undergo minimally invasive augmentation or rejuvenation of the face. Treatments with dermal fillers can create a more youthful appearance with immediate and predictable results and a short recovery time. It is crucial that filler materials be placed in the subcutaneous tissue, in the spaces between the periosteum and muscle, or between muscle fibers, as deemed appropriate for the anatomical site (Cong et al., 2016; Tansatit et al., 2017).

Filler injection into the forehead without topographic knowledge of the underlying structures may result in accidental puncture of the vasculature and migration of the filler into blood vessels. For the glabellar augmentation, it has been recommended that the cannula should be inserted from the midline of upper forehead and proceed retrograde injection by fanning technique (Kim et al., 2016). As a result, filler particles are not easily injected into the vessels. However, filler products may cause the skin necrosis due to the blocking the blood pathway by the compression of the arterial structures. Filler particles can be directly injected into the Fbrs of OA and it can cause the intravascular occlusion, and rarely leading to severe blindness (Wu et al., 2017; Kim et al., 2016; Li et al., 2015; Maruyama, 2017).

The pretarsal roll is the bulged margin of the lower eyelid above the pretarsal groove. This region is formed by the contraction of the orbicularis oculi when smiling and is more distinct in young people. Many Asian patients regard the pretarsal roll as youthful and attractive. Consequently, filler injections to augment the pretarsal roll have become popular in Asian

countries. Injection of fillers near the pretarsal part of the lower eyelid may result in vision loss by interfering with the IMPA, a branch of the OA that supplies the lower eyelid. The filler droplet was observed as an intervascular remnant after injection of the filler by histopathologic investigation (Kim et al., 2014). However, guidelines specifying the appropriate depths for filler placement are lacking because the topographic anatomy of the face has not been fully characterized.

The upper eyelid myocutaneous flap (UEMF) has been used as oculoplastic surgical techniques for periorbital tissue defect reconstruction as it provides advantages such as no color differences and no long-term donor scar after a simple operation. The UEMF including the emerging point of the OA (EMP of OA) and its branches ensures a maximal blood supply which is closely linked to the success of flap surgeries (Chang, 2017; Frederic, 2013; Han et al., 2015; Kim et al., 2012; Tirone et al., 2009).

Therefore, the aims of this study were (1) to determine the three-dimensional (3D) location of the EMP of OA inferior to the SOR, (2) to establish a detailed topography of the forehead vasculature including the branching and distribution patterns of the STA and the supraorbital artery (SOA), and (3) to perform a topographic analysis of the distribution patterns and diameters of the IMPA, thereby providing the clinical guidelines for safe performances of periorbital minimally-invasive and surgical procedures.

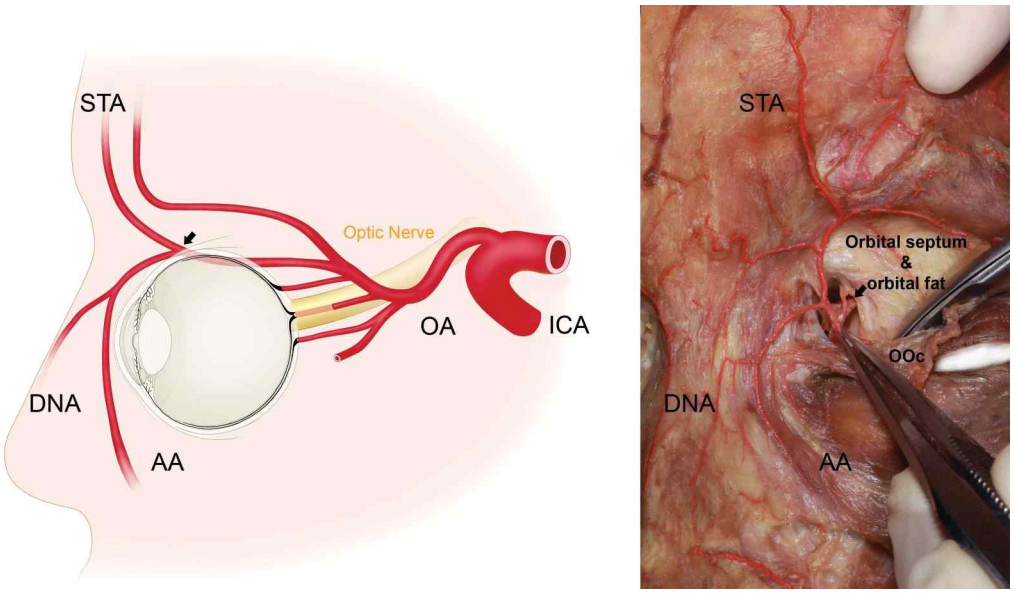

Figure 1. Illustration of the emerging point of ophthalmic artery (EMP of OA). Left panel: A lateral view of the whole courses of the OA. Right panel: An anterior view via a cadaver dissection of the EMP of OA. The EMP of OA pierced the orbital septum and the orbicularis oculi (OOc) until it divided into several branches. Black arrowheads indicate the EMP of OA. ICA, interal carotid artery; STA, supratrochlear artery; DNA, dorsal nasal artery; AA, angular artery.

Ⅱ. MATERIALS & METHODS

1. Materials

Latex (Neoprene, lot no. 307L146; DuPont DeNemours, Puteaux, France) containing a red and blue colorant (Castorama, Templemars, France) was injected into the common carotid artery and internal jugular vein to enable clear visualization of the vascular structures. All of those studies were performed in accordance with the principles outlined in the Declaration of Helsinki. Appropriate consent and approval were obtained from the families of the cadavers before the dissections were performed and from volunteers themselves before the ultrasound detections were performed.

PART I: Three-dimensional (3D) identification of the emerging point of ophthalmic artery (EMP of OA)

The EMPs of OA of 17 hemifaces (11 males, 6 females; mean age, 80) from 10 Korean cadavers (7 males, 3 females; mean age, 77) and 7 Thai cadavers (4 males, 3 females; mean age, 83) were serially dissected and scanned by 3D scanner (Morpheus3D®, Morpheus Company, Seongnam, Korea). In addition, the EMPs of OA of 30 healthy Korean volunteers (18 males, 12 females; mean age, 26) were detected by an ultrasound device (E-CUBE15, ALPINION, Seoul, Korea).

PART II: Arterial distribution of the forehead

The STA and the SOA were evaluated in 20 hemifaces from one Korean and 10 Thai cadavers (7 males, 4 females; mean age, 75) to map the arterial system of the forehead. There were nine cadavers that were dissected on both

sides and two cadavers that were dissected on only one side because of the unclear injected vascular structures on the other side.

PART III: Anatomic location and courses of the inferior medial palpebral artery (IMPA)

IMPAs were examined in 31 hemifaces from 13 Korean and eight Thai cadavers (15 males and 6 females: mean age, 85). Thirty hemifaces underwent dissection, and one hemiface underwent histologic analysis. Eight cadavers were dissected on only one side because of the poor vascular structures on the other side, and 11 cadavers were dissected on both sides.

2. Methods

PART I: Three-dimensional (3D) identification of the emerging point of ophthalmic artery (EMP of OA)

1) Cadaveric dissection and 3D scanning for detecting the location of EMP of OA:

The 3D scanning and anatomical dissection were proceeded according to Lee et al. (2017). The first 3D scanning was performed prior to dissection to capture the whole skin surface of the cadaver. It was scanned from the frontal and bilateral oblique aspects by structured-light 3D scanner (Morpheus3D®, Morpheus Company, Seongnam, Korea). The scanned face was reconstructed using Morpheus Plastic Solution (version 3.0) software (MPS 3.0; Morpheus Company). The 3D scanned images from the frontal and bilateral oblique aspects of the face were combined and merged through geometry analysis of the nearby areas at three points (lateral canthus, alare and cheilion) bilaterally. After skin surface scanning, the dissections on the left side of the specimen

face slightly deviating right of the midline were performed. According to the different facial structures: skin, orbicularis oculi muscle, and soft tissue surrounding the EMP of OA were removed in serial manner. Special attention was paid to ensure that the EMP of OA and its branches were not damaged or deformed. The EMP of OA, the medial canthus (MC) and the inferior margin of the SOR were identified after the dissection. After exposure of the EMP of OA, the specimen was scanned again. The undissected right portion of the specimen face was preserved for later use as a landmark for superimposition procedure. Finally, the first undissected image and second half dissected image including the EMP of OA were superimposed based on the preserved side of the face by using MPS system. In terms of the depth measurement from the skin to the EMP of OA, it was performed both in specimens by 3D scanning and in volunteers by US imaging systems.

In addition, another four parameters were measured by MPS program to detect the location of the EMP of OA based on different landmarks as follows (Fig. 3):

From the MC coordinate, 1) the transverse distance from the MC to the EMP of OA and 2) the vertical distance from the MC to the EMP of OA were measured. Based on the facial sagittal midline (FSM), 3) the transverse distance from the FSM to the EMP of OA and 4) the transverse distance from the FSM to the MC were measured.

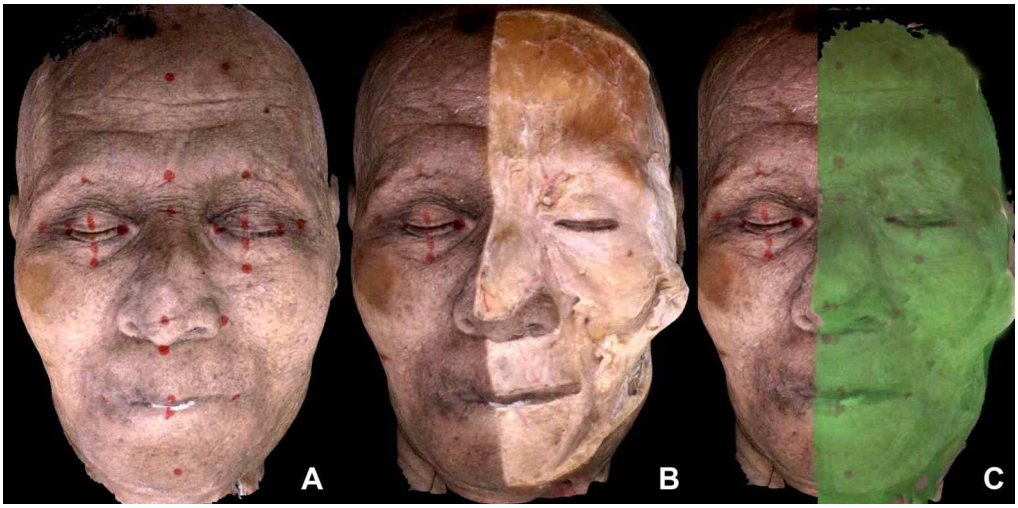

Figure 2. Superimposition of three-dimensional (3D) reconstructed images from two different layers by Morpeus Plastic Solution (MPS) program. A: First 3D scanned image of the skin surface prior to dissection. B: Second 3D scanned image of the EMP of OA after serial dissections. C: The images of A and B were aligned and superimposed based on the preserved side of the face using MPS 3.0. The dissected area on the superimposed face is indicated in green color.

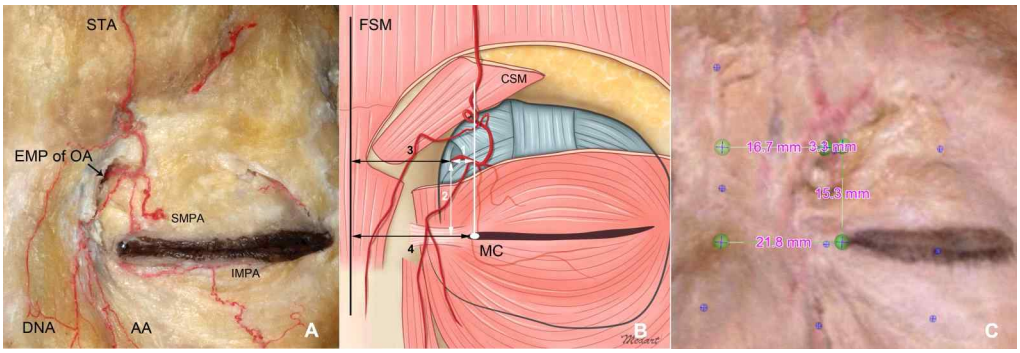

Figure 3. Identification of the emerging point of ophthalmic artery (EMP of OA) by Morpheus Plastic Solution (MPS) program. A: Image of the EMP of OA and its branches via a dissected cadaver. B: Schematic diagram of measurements: 1) the transverse distance from the medial canthus (MC) to the EMP of OA and 2) the vertical distance from the MC to the EMP of OA, 3) the transverse distance from the facial sagittal midline (FSM) to the EMP of OA and 4) the transverse distance from the FSM to the MC. C: Template image of the measurement performed by MPS program. DNA, dorsal nasal artery; AA, angular artery; SMPA, superior medial palpebral artery; IMPA, inferior medial palpebral artery; STA, supratrochlear artery; CSM, corrugator supercilii muscle.

2) Ultrasound (US)-based identification of the location of the emerging point of ophthalmic artery (EMP of OA)

For the US-based detection of the EMP of OA, volunteers were all placed in the supine position, and the US gel was applied softly above the upper eyelid skin surface with little bubbles. The detect transducer (model I08-17) was located vertically, and the center of it was placed at the meeting point between the transverse SOR plane and the vertical MC plane. The periorbital anatomic structures were first detected by ultrasound in black-and-white image and were confirmed by muscle contraction of the volunteers. Then the doppler function was used to detect the vascular course in red-and-blue colors, and finally the pulse function was used to detect the EMP of OA in wave shapes. Additionally, there were two parameters measured by an image analysis program (Image J, National Institutes of Health, Bethesda, MD, USA) via US images to detect the location of the EMP of OA as follows (Fig. 4):

a: the depth from the skin to the EMP of OA; b: the vertical distance from the inferior margin of the SOR to the EMP of OA.

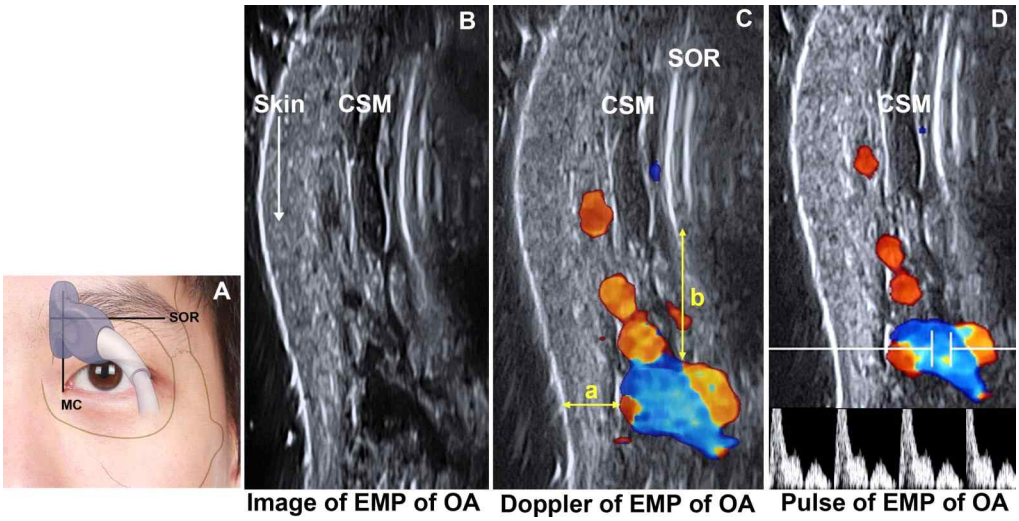

Figure 4. Detection of the emerging point of ophthalmic artery (EMP of OA) by ultrasound (US) imaging system. A: The US detect transducer was located vertically, and the center of it was placed at the meeting point between the transverse superior orbital rim (SOR) plane and the vertical medial canthus (MC) plane. B: The detected image of periorbital structures showed in black-and-white colors. C: The doppler-detected image showed the vascular course in red-and-blue colors. D: The wave-pulse-detected image indicated the EMP of OA. CSM, corrugator supercilii muscle.

PART II: Arterial distribution of the forehead

The skin and subcutaneous tissues then were removed, and meticulous dissection was performed to reveal the vascular structures. Overlying muscles were cut and retracted as needed to expose the entire courses of the STA and the SOA. The superficial and deep branches of the STA and the SOA were defined as the arterial structures along the regions superficial or deep to the frontalis, respectively.

Several reference planes and landmarks were noted to facilitate the topographic analysis (Fig. 5). The horizontal plane through the palpebral fissure from the MC to the lateral canthus was designated X1. The horizontal plane through the supraorbital margin, parallel to X1, was deemed X2. The vertical plane through the MC, perpendicular to X1 and X2, was designated Y. The supraorbital foramen (SOF) was mapped relative to X1 and Y. The site of penetration of the deep branch of the SOA (dSOA) on the frontalis was mapped relative to X2 and Y.

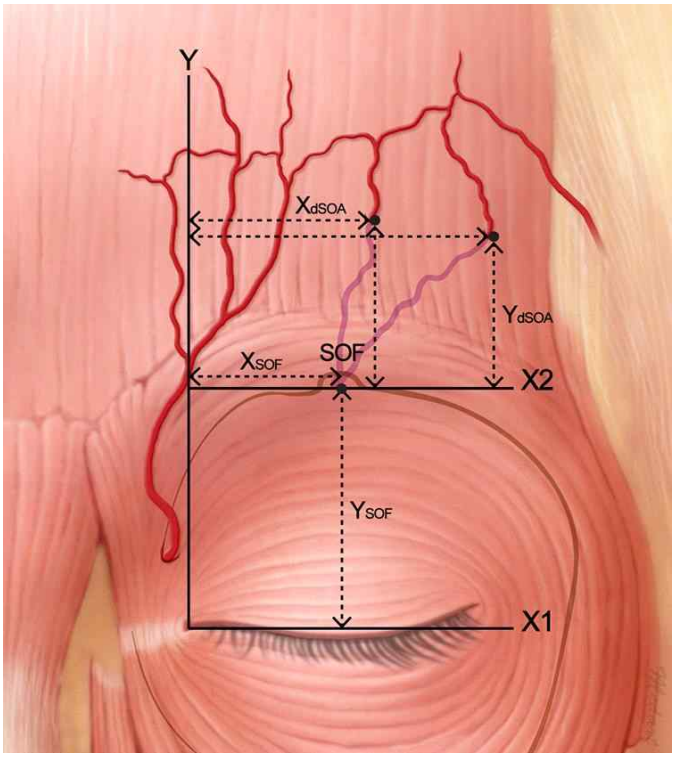

Figure 5. Reference planes and landmarks for the forehead arterial system. X1, the horizontal plane through the palpebral fissure from the medial canthus to the lateral canthus. X2, the horizontal plane through the supraorbital margin, parallel to X1. Y, the vertical plane through the medial canthus, perpendicular to X1. X_{SOF}: horizontal distance of the supraorbital foramen (SOF) on the plane X2 from the plane Y, Y_{SOF}: vertical height of the SOF from the plane X1; X_{dSOA}: average horizontal distance of the penetration point on the frontal is of the deep branch of the supraorbital artery (dSOA) from the plane Y, Y_{dSOA}: average vertical height of the penetration point on the frontalis of the dSOA from the plane X2. The superficial branch of the supratrochlear artery and the superficial branch of the supraorbital artery are depicted in red; the dSOA is in violet.

PART III: Anatomic location and courses of the inferior medial palpebral artery (IMPA)

The skin and orbicularis oculi were removed by meticulous dissection to reveal the IMPA. The distribution patterns of the IMPA were determined in relation to the SMPA and the STA into four types (Fig. 6): type I, the IMPA and the SMPA individually branched from the OA with the OA terminating as the STA on the forehead; type II, a short trunk arose from the OA and subsequently branched into the IMPA and the SMPA, with the OA terminating as the STA; type III, the IMPA and the SMPA branched together from the OA, and the OA terminated as the STA; or type IV, the IMPA and the SMPA constituted the terminal branches of the OA, with the STA arising from the AA.

For each hemiface, the IMPA was mapped according horizontal (*X*) and vertical (*Y*) coordinates and relative to surface landmarks, including the MC and the lateral canthus (LC; Fig.7). The X axis was defined as the transverse plane along the palpebral fissure from the MC to the LC. The Y axis extended in the sagittal plane through the MC. The topography of the IMPA in the lower eyelid was determined at the entry point into the lower eyelid (*a*; Fig.7); the inflection point along the tarsal plate of the lower eyelid (*b*); and the ending point (*c*). When the IMPA ran the entire length along the tarsal plate in the lower eyelid, the c point was measured at the LC(c_l); when the IMPA penetrated the tarsal plate before reaching the LC, the c point was measured at the penetration point (c_p). The diameter of the IMPA was determined at points *a* and *c* (c_l and c_p). For a microscopic assessment of the IMPA, a specimen from 1 hemiface was embedded in paraffin and sectioned for histologic processing by conventional methods.

All measurements were made with digital calipers (CD-15CP, Mitutoyo, Kanagawa, Japan), and data were represented as mean±standard deviation

(SD). A P value<0.05 was considered significant via an independent t test.

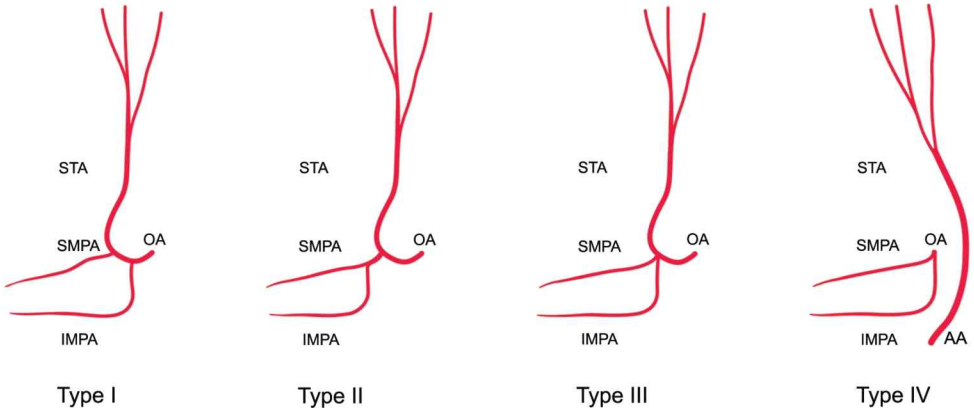

Figure 6. Schematic diagrams of the 4 distribution patterns formed by the inferior medial palpebral artaery (IMPA) relative to the superior meidal palpebral artery (SMPA) and the supratrochlear artery (STA). Type I: The IMPA and SMPA branched from the ophthalmic artery (OA) individually with the OA terminating as the STA on the forehead. Type II: A short, common trunk branched from the OA and divided into the IMPA and SMPA; the OA terminated as the STA. Type III: The IMPA and SMPA branched from the OA at the same point, and the OA terminated as the STA. Type IV: The IMPA and SMPA constituted the terminal branches of the OA; the STA arose from the angular artery (AA).

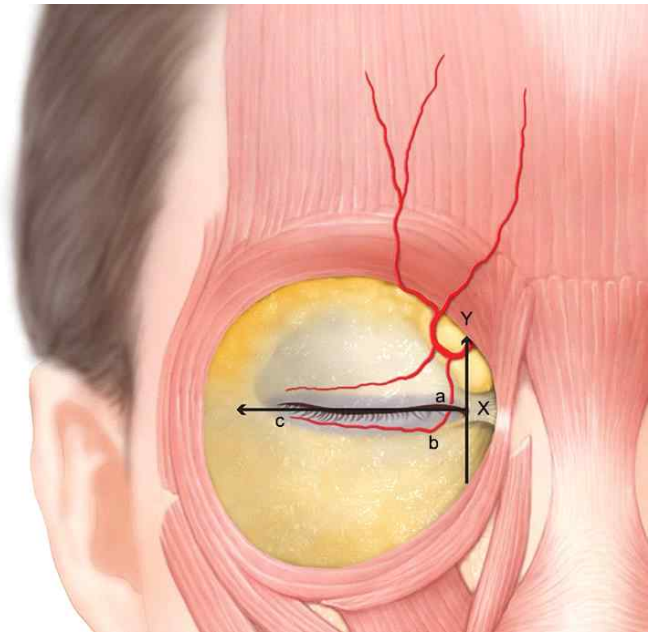

Figure 7. Evaluation of the course of the inferior medial palpebral artery (IMPA) in the lower eyelid relative to a plane defined by horizontal (X) and vertical (Y) axes through the medial canthus (MC). The X axis corresponded to the transverse plane along the palpebral fissure from the MC to the lateral canthus (LC). The Y axis corresponded to the sagittal plane perpendicular to the X axis through the MC. The location of the IMPA was measured at 3 points: *a*, the entry point into the lower eyelid; *b*, the inflection point along the tarsal plate of the lower eyelid; and *c*, the ending point. The diameter of the IMPA was determined at points *a* and *c*. (c_l and c_p). When the IMPA ran the entire length of the tarsal plate in the lower eyelid, the c point was measured at the LC (c_l); when the IMPA penetrated the tarsal plate before reaching the LC, the c point was measured at the penetration point (c_p).

Ⅲ. RESULTS

PART I: Three-dimensional (3D) identification of the emerging point of ophthalmic artery (EMP of OA)

On 17 sides of the superimposed 3D scan images using MPS program, the location of the EMP of OA based on different facial landmarks were identified and measured. From the MC coordinate, the transverse distance to the EMP of OA was 3.8±1.0 mm medially, and the vertical distance was 14.0±2.9 mm superiorly, respectively. From the FSM, the transverse distance to the EMP of OA was 16.5±1.7 mm and 20.0±2.0 mm to the MC, respectively (Fig. 8).

Secondly, the locations of the EMP of OA of 30 volunteers' were observed by US images and measured by an Image J program. Anatomic periorbital structures were confirmed by following serial steps: US image, doppler and pulse functions via a US imaging device. The vertical distance was 5.3±1.4 mm from the inferior margin of the SOR to the EMP of OA (Fig. 9).

Thirdly, the in-depth measurements were performed from the skin to the EMP of OA on specimens and volunteers using superimposed 3D scanned images and US images, respectively. After detecting the specimens via 3D scanned images, the depth was measured at 4.8±1.7 mm below the skin to the EMP of OA; after detecting the volunteers with US images, the depth was measured to be 4.5±1.1 mm below the skin to the EMP of OA (Fig. 9 and Table. 1). There were no statistically significant differences in terms of the depth from the skin to the EMP of OA between 3D scanning and US imaging systems. The depth data showed that 4.5±1.3 mm and 4.6±1.0 mm in males and females, respectively. There were no statistically significant differences between sexes in depth from the skin to the EMP of OA.

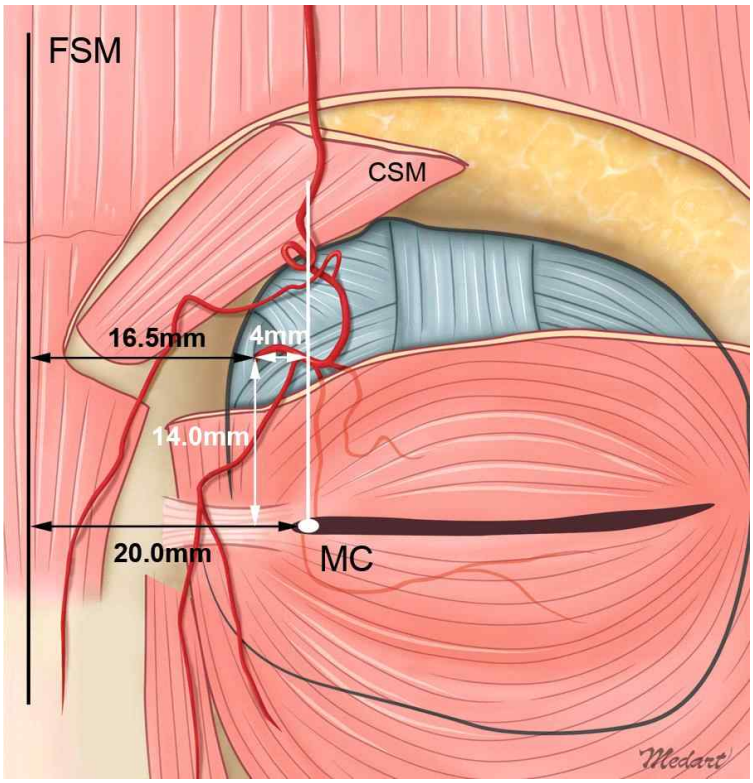

Figure 8. Location of the emerging point of ophthalmic artery by Morpheus Plastic Solution measurement. MC, medial canthus; FSM, facial sagittal midline; CSM, corrugator supercilii muscle.

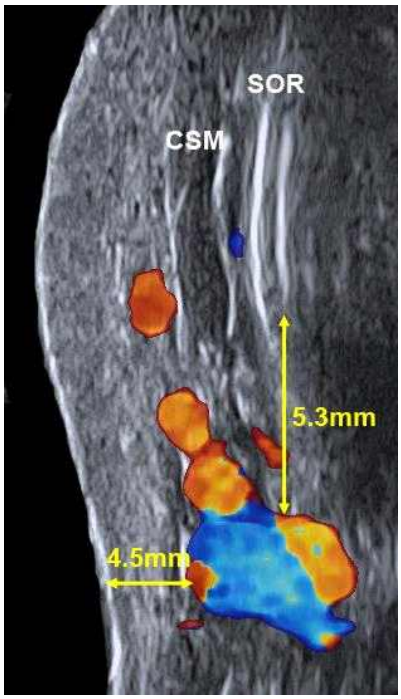

Figure 9. Location of the emerging point of ophthalmic artery by ultrasound detection. CSM, corrugator supercilii muscle; SOR, superior orbital rim.

Table 1. Depth measurements from the skin to the emerging point of ophthalmic artery (EMP of OA) (mean±SD, mm).

Measurement methods	Depth from skin to the EMP of OA
3D scanning	4.8±1.7
Ultrasound detection	4.5±1.1

SD, standard deviation

PART II: Arterial distribution of the forehead

The superficial branch of the STA (sSTA), the superficial branch of the SOA (sSOA), and the dSOA were observed in all of the specimens.

Two arterial distribution patterns of the forehead were classified whether the deep branch of the STA (dSTA) was present or not (Fig. 10). The type I (dSTA-present pattern, 11 of 20 cases; 55%) comprised two subtypes: For the type Ia (7 of 20 cases, 35%), the layer superficial to the frontalis was supplied medially by sSTA and laterally by the sSOA; the dSTA and the dSOA were distributed deep to the frontalis. For the type Ib (4 of 20 cases; 20%), the layer superficial to the frontalis was supplied by the sSTA and the sSOA in addition to the central artery or the paracentral artery; the dSTA and dSOA supplied the layer deep to the frontalis. For the type II (dSTA-absent pattern, 9 of 20 cases; 45%), the layer superficial to the frontalis was supplied medially by the sSTA and laterally by the sSOA; only the dSOA supplied the layer deep to the frontalis (Figs. 10 and 11). Among 9 specimens dissected on both sides, 7 out of 9 were shared the same arterial distribution type on both sides. One out of the left 2 specimens was shared the type II on right side and type Ia on left side; the other specimen was shared the type II on right side and type Ib on left side.

For all cases, the SOA originated deep to the frontalis (ie, dSOA), extended superolaterally from the SOF, and penetrated the frontalis to become the sSOA. The mean±SD coordinates of this penetration point were 29.6±4.1 mm horizontally from Y, and 20.7±5.1 mm vertically from X2. The SOF was localized 10.8±4.9 mm horizontally from Y and 22.1±2.6 mm vertically from X1 (Tables 2 and 3). When the data were stratified by gender, there were no significant differences between the measurements.

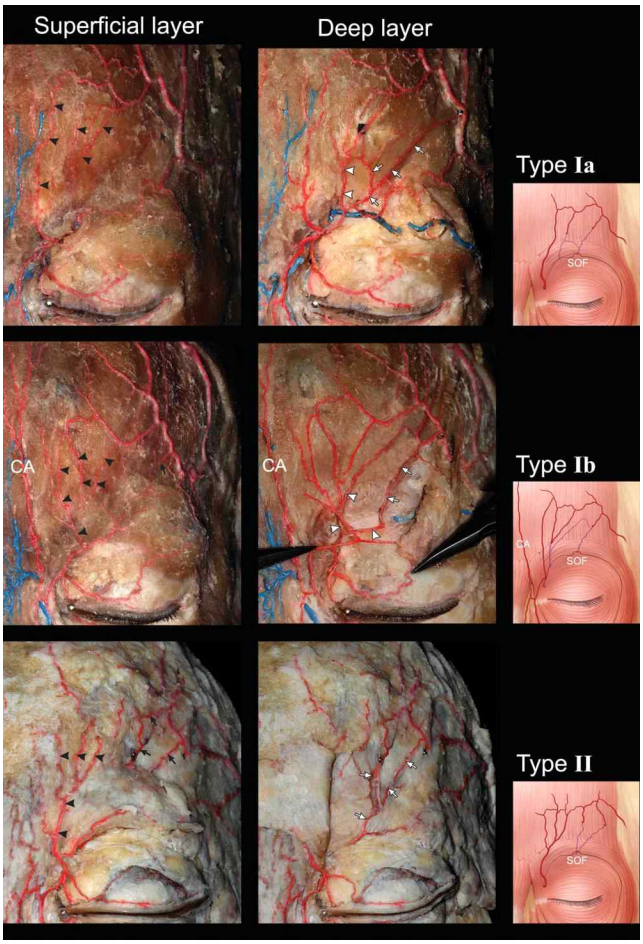

Figure 10. Two arterial distribution patterns of the forehead. The type I [deep branch of supratrochlear artery (dSTA) present pattern, 11 of 20 cases; 55%] constituted two subtypes: For the type Ia (7 of 20 cases, 35%), the layer superficial to the frontalis was supplied medially by superficial branch of supratrochlear artery (sSTA) and laterally by the superficial branch of supraorbital artery (sSOA); the dSTA and the deep branch of supraobrital artery (dSOA) were distributed deep to the frontalis. For the type Ib (4 of 20 cases; 20%), the layer superficial to the frontalis was supplied by the sSTA and the sSOA in addition to the central artery (CA) or the paracentral artery;

the dSTA and dSOA supplied the layer deep to the frontalis. For the type II (dSTA-absent pattern, 9 of 20 cases; 45%), the layer superficial to the frontalis was supplied medially by the sSTA and laterally by the sSOA; only the dSOA supplied the layer deep to the frontalis. Left panels, dissected areas superficial to the frontalis, black arrowheads and black arrows indicate sSTA and sSOA, respectively; middle panels, dissected areas deep to the frontalis, white arrowheads and white arrows indicate dSTA and dSOA, respectively; right panels, schematic arterial distributions (SOF: supraorbital foramen).

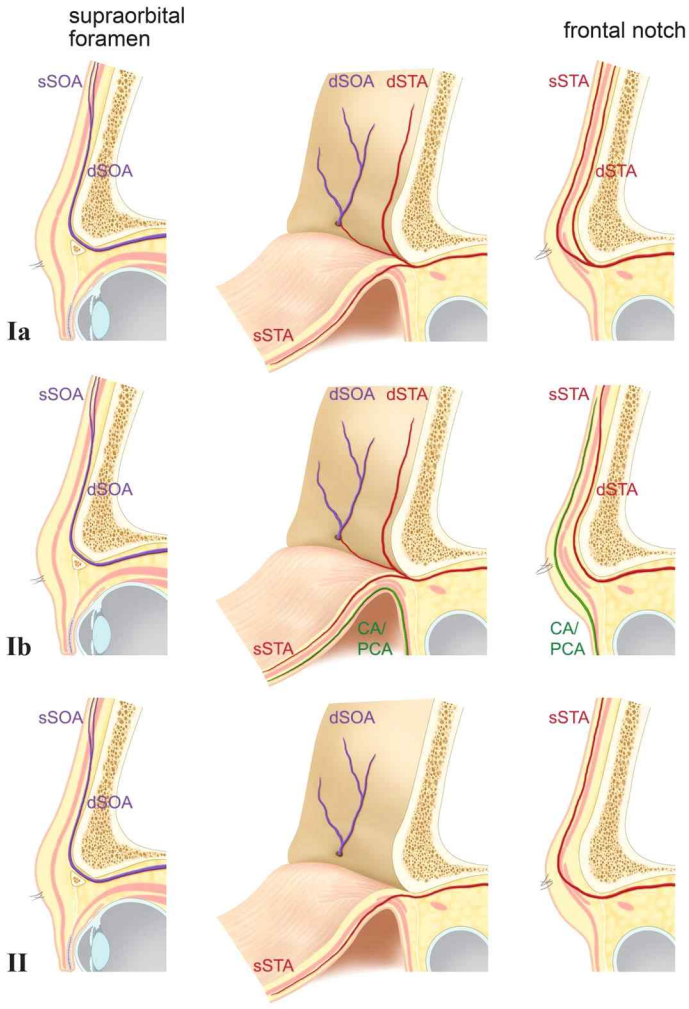

Figure 11. Schematic sagittal views of the two main arterial distribution patterns of the forehead with the skin to frontalis retracted on the middle panels. Left and right panels show the sagittal section along the supraorbital foramen and the frontal notch, respectively. For the type Ia the layer superficial to the frontalis was supplied medially by superficial branch of supratrochlear artery (sSTA) and laterally by the superficial branch of supraorbital artery (sSOA); the deep branch of supratrochlear artery (dSTA)

and the deep branch of supraobrital artery (dSOA) were distributed deep to the frontalis. For the type Ib, the layer superficial to the frontalis was supplied by the sSTA and the sSOA in addition to the central artery (CA) or the paracentral artery (PCA); the dSTA and dSOA supplied the layer deep to the frontalis. For the type II , the layer superficial to the frontalis was supplied medially by the sSTA and laterally by the sSOA; only the dSOA supplied the layer deep to the frontalis.

Table 2. Coordinates of the penetration point on the frontalis of the deep branch of the supraorbital artery (dSOA) (mean±SD, mm)

	X_{dSOA}	Y_{dSOA}
Right hemifaces (N = 10)	28.4±10.1	16.0±5.2
Left hemifaces (N = 10)	25.9±10.3	24.4±7.9
Overall (N = 20)	29.6±4.1	20.7±5.1

SD, standard deviation

Table 3. Coordinates of the supraorbital foramen (SOF) (mean±SD, mm)

	X_{SOF}	Y_{SOF}
Right hemiface (N = 10)	9.7±4.3	21.9±2.8
Left hemiface (N = 10)	11.9±5.4	22.3±2.6
Overall (N = 20)	10.8±4.9	22.1±2.6

SD, standard deviation

PART III: Anatomic location and courses of the inferior medial palpebral artery (IMPA)

For all specimens, the IMPA and the SMPA branched from the OA, and the distribution of the IMPA corresponded to 1 of 4 patterns (Fig. 12): Of the 30 hemifaces examined, distribution patterns I, II, III, and IV were observed in 11 hemifaces (36.7%), 11 hemifaces (36.7%), 7 hemifaces (23.3%), and 1 hemiface (3.3%), respectively. The IMPA extended inferolaterally after branching from the OA and subsequently entered the lower eyelid lateral to the MC through a space. This space was filled with septal fat and was located deep to the OOc (Fig. 13).

Two extensions of the IMPA at the lower eyelid were observed. In 21 of the 30 dissected hemifaces (70.0%), the IMPA extended the entire length of the tarsal plate of the lower eyelid and anastomosed with the lateral palpebral artery of the lacrimal artery at the LC (type A; Fig. 14). In 9 hemifaces (30.0%), the IMPA penetrated the tarsal plate before reaching the LC (type B). The penetration points were variable, occurring in the medial third (3 of the 9 hemifaces), middle third (2 of 9 hemifaces), or lateral third (4 of 9 hemifaces) of the tarsal plate. The results of histologic analysis indicated that the IMPA was positioned between the pretarsal part of the OOc and the lower border of the tarsal plate (Fig. 15).

The coordinates of the IMPA at the 3 reference points (ie, *a*, the entry point into the lower eyelid; *b*, the inflection point along the tarsal plate of the lower eyelid; and *c*, the ending point) are presented in Table 4. The IMPA tapered from the MC to the LC. The diameter of the IMPA was 0.94±0.22 mm at *a*, 0.37±0.11 mm at the c_l, and 0.35±0.11 mm at the c_p (Table. 5). The diameters of the IMPA for extension types A and B were not significantly different.

Ten out of 11 cadavers in which both hemifaces were dissected and the features of the IMPAs on the right and left sides were the same. One out of

the 11 cadavers in which the hemifaces differed was classified as type III on the right side and type I on the left side. The topography and branching patterns of the IMPAs did not differ significantly by gender or ethnicity.

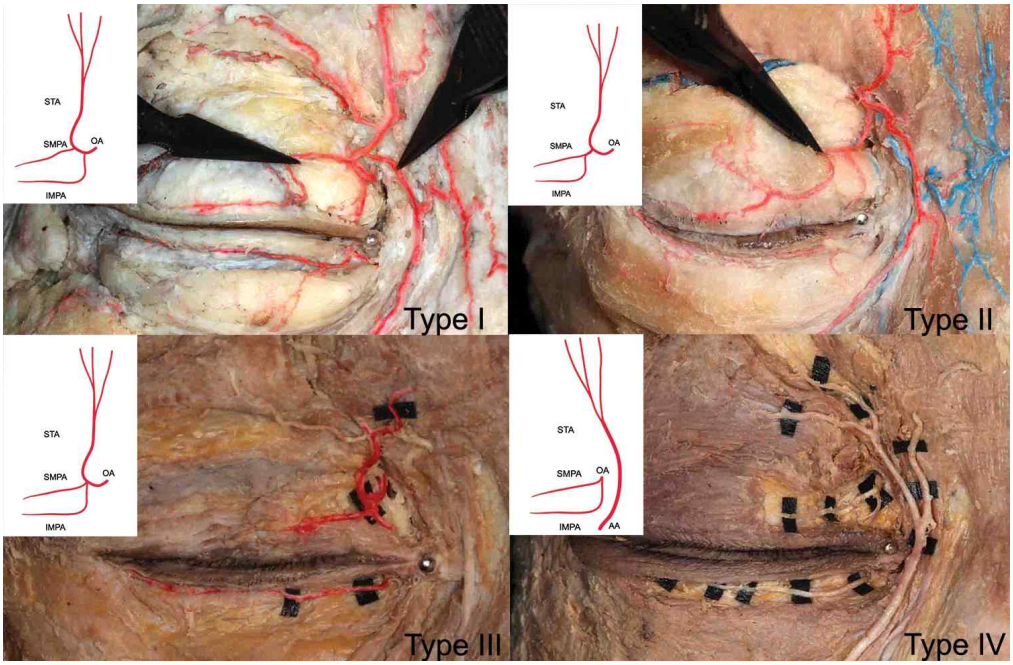

Figure 12. Four distribution patterns formed by the inferior medial palpebral artery (IMPA) relative to the superior medial palpebral artery (SMPA) and the supratrochlear artery (STA). Insets depict the schematic diagrams presented in Figure 6. Types I and II each were observed in 11 of the 30 dissected hemifaces (36.7% each). Type III was observed in 7 hemifaces (23.3%). Type IV was observed in 1 hemiface (3.3%). OA, ophthalmic artery; AA, angular artery.

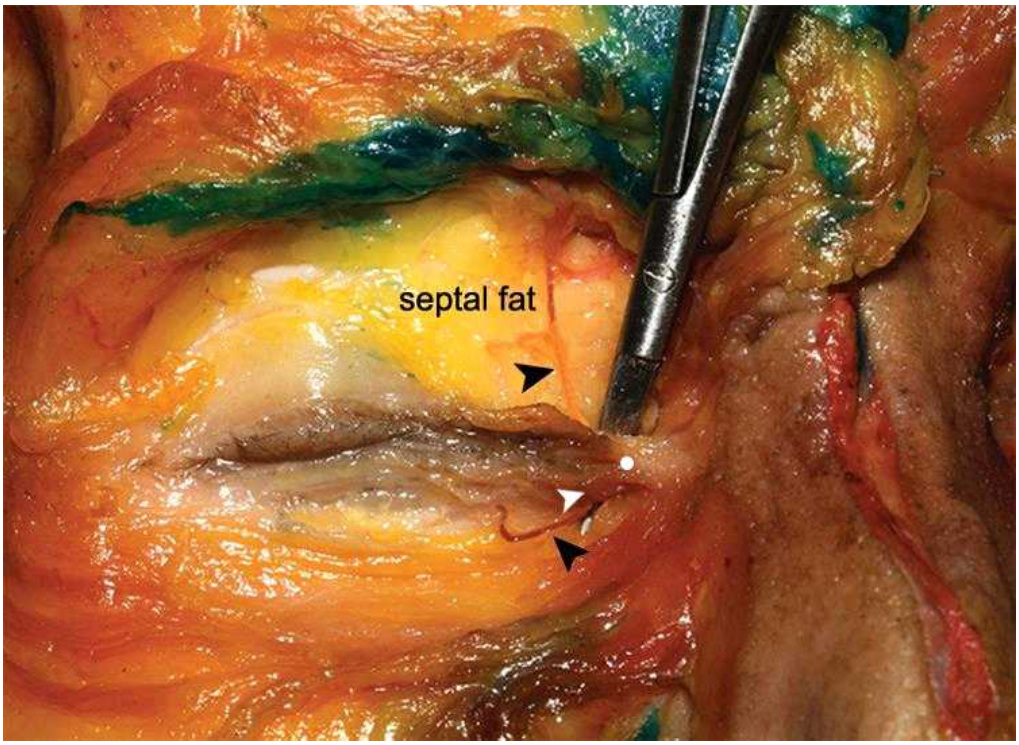

Figure 13. The space into which the inferior medial palpebral artery (IMPA) entered the lower eyelid. Cadaver dissections indicating the space was lateral to the medial canthus and deep to the orbicularis oculi muscle. Scissors have been inserted through the space. The two black arrowheads indicate the IMPA. The white arrowhead indicates the pretarsal part of the orbicularis oculi muscle. The white point indicates the medial canthus.

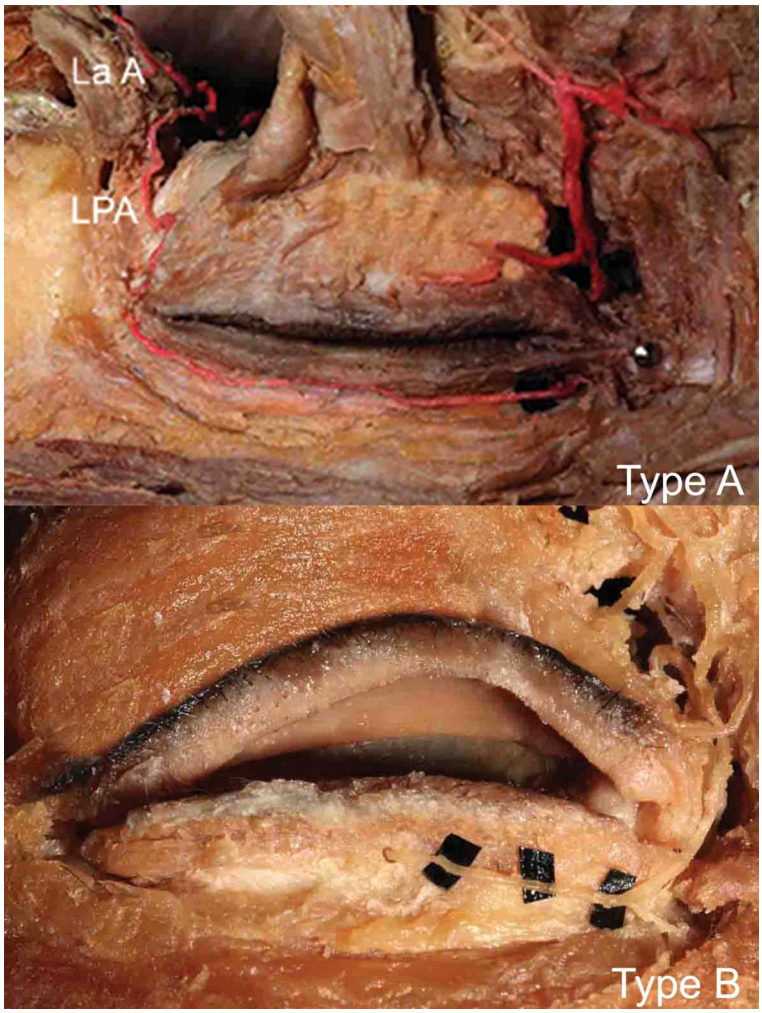

Figure 14. Two extensions of the inferior medial palpebral artery (IMPA) in the lower eyelid. In type A [21 of the 30 dissected hemifaces (70.0%)], the IMPA ran the entire length of the tarsal plate of the lower eyelid and anastomosed with the lateral palpebral artery (LPA) of the lacrimal artery (La A) at the lateral canthus. In type B [9 hemifaces (30.0%)], the IMPA penetrated the tarsal plate before reaching the lateral canthus.

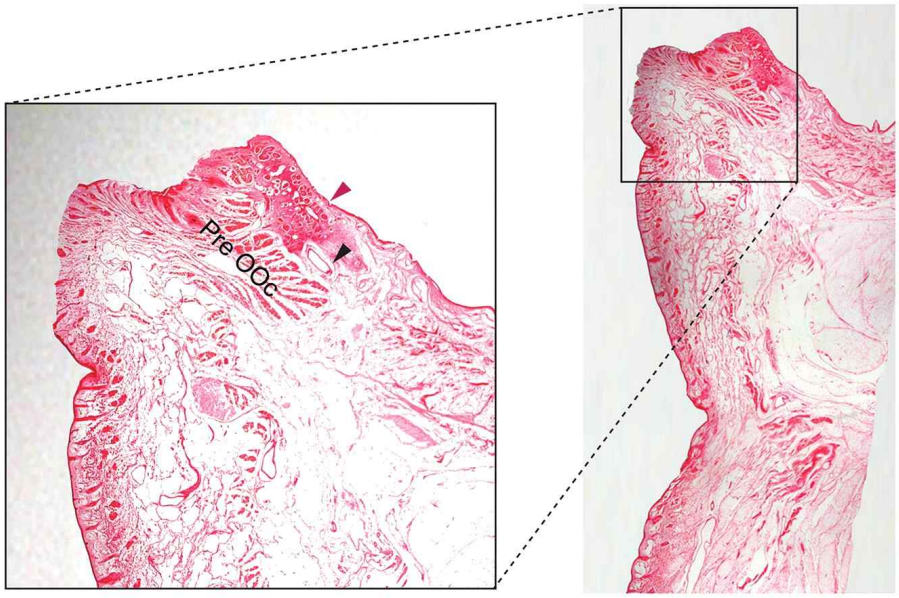

Figure 15. Sagittal section of the inferior medial palpebral artery (IMPA) processed with conventional histologic methods. The IMPA (black arrowhead) is located between the pretarsal part of the orbicularis oculi (Pre OOc) and the lower level of the tarsal plate (red arrowhead). The leftmost and rightmost margins of the section correspond to the skin and the tarsal plate, respectively. The square area in the right panel was magnified in the left.

Table 4. Coordinates of the inferior medial palpebral artery (IMPA) in the lower eyelid (mean±SD, mm).

	X	Y
a, entry point	3.69±1.06	0.00
b, inflection point	5.08±1.57	-4.10±1.03
c_l, lateral canthus	30.68±4.06	-2.36±0.79
c_p, penetration point	17.73±4.56	-3.64±0.89

SD, standard deviation

X: the transverse distance from the IMPA to the medial canthus

Y: the vertical distance from the IMPA to the palpebral fissure

c_l: when the IMPA ran the entire length along the tarsal plate in the lower eyelid, the point c was measured at the lateral canthus;

c_p: when the IMPA penetrated the tarsal plate before reaching the lateral canthus, the point c was measured at the penetration point.

("-" a negative value indicated that the IMPA was located below the palpebral fissure)

Table 5. Diameter of the inferior medial palpebral artery (IMPA) at the entry point and the ending point (mean±SD, mm).

	Diameter of the IMPA
a, entry point	0.94±0.22
c_l, lateral canthus	0.37±0.11
c_p, penetration point	0.35±0.11

SD, standard deviation

c_l: when the IMPA ran the entire length along the tarsal plate in the lower eyelid, the ending point c was measured at the lateral canthus;

c_p: when the IMPA penetrated the tarsal plate before reaching the lateral canthus, the ending point c was measured at the penetration point.

Ⅳ. DISCUSSION

The OA exits and emerges at the orbital region by piercing the orbital septum inferior to the medial portion of SOR; it then divides into several facial braches: the STA which supplies the forehead; the SMPA and IMPA which supply the upper and lower eyelids, respectively. During the past decades, numerous authors have examined the facial branches of the OA (Fbrs of OA), including the STA and the SOA, in the context of facial reconstruction surgery. (Fukuta et al., 1994; Yoshioka and Rhoton, 2005; Erdogmus and Govsa, 2017). The detailed anatomic description on the emergence and vascular distribution of the Fbrs OA are not known, despite of the wide variety of clinical applications such as filler injections and UEMFs.

The present study yielded the first anatomical report on 3D location where the OA exited and emerged using 3D scanning and US imaging systems. Moreover, it provided clinicians with topographic distributions of the STA and SOA on forehead and anatomic courses of the IMPA along the tarsal plate of the lower eyelids, following an emergence of the OA.

PART I: Three-dimensional (3D) identification of the emerging point of ophthalmic artery (EMP of OA)

3D scanning system is well applied to the aesthetic and dental solutions to ultimately assist surgeons in making diagnostic and treatment evaluations. A white light-emitting diode was used as a low-power visible-light source in the scan imaging unit. Therefore, images can be acquired without harming the subject's eyes. The manufacturer claimed that the spatial accuracy was better than 0.1 mm. It took approximately 0.8 seconds to complete the entire scanning procedure and the images were obtained at three different horizontal angles

(the frontal and bilateral oblique aspects of the face). Because of its higher accuracy and fewer subtlety losses, the 3D scanning system has already substituted the traditionally two-dimensional photograph analysis. Therefore, 3D scanning system was commonly used in literatures for various medical purposes: detection of skin thickness, evaluation of facial blood flow, and calculation of volume and topographic distances as well as facial angles (Rho et al., 2017; Zhao et al., 2017; Bock et al., 2017). The present study performed an in-depth measurement on cadavers by 3D MPS system and it was 4.8±1.7 mm from the skin to the EMP of OA. Based on the data we got by 3D scanning system measurement, the 3D location of the EMP of OA can be located by one thumb finger-width above and 4mm medial to the MC coordinate, in addition to a 5mm depth from the skin (Fig. 16).

Medical US devices have been widely used in clinical diagnosis, fetal detection and injection guiding for their advantages of being non-invasive, cheap and fast, etc (Han et al., 2015; Zheng et al., 2015; Chaves et al., 2017; Arnuntasupakul et al., 2017; Kariya et al., 2017). Despite of the prevalence of US application, there is still dearth of references for facial parts detection. Doppler and pulse functions were performed in this study to detect the EMP of OA on volunteers by a US device. It was 5.3±1.4 mm from the inferior margin of SOR to the EMP of OA vertically. If there was a MC defect, surgeons could use the FSM as another alternative to identify the EMP of OA: The transverse distance was 16.5 mm from the EMP of OA to the FSM as well as the EMP of OA emerging at a 5.3 mm vertical distance inferior to the SOR. Moreover, it was 4.5±1.1 mm in depth from the skin to the EMP of OA.

This study provided objective data regarding the 3D location of the EMP of OA by 3D scanning and US imaging systems both in cadavers and volunteers, respectively. These results may contribute to the incipient knowledge of the

EMP of OA. With the aforementioned-data, the clinicians can use the thumb and index fingers to press the location of EMP of OA during the periorbital filler injection procedures, avoiding unintended vascular piercing. The surgeons could perform accurate oculoplastic surgeries when obtain the effective vascularization for a UEMP, avoiding iatrogenic bleeding at the operation site. The results of this study may possibly improve periorbital clinical interventions.

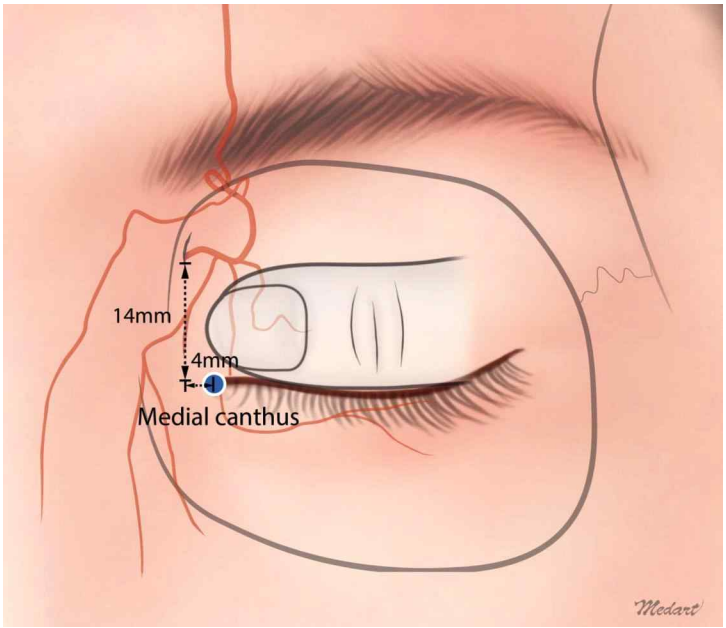

Figure 16. Schematic diagram of the three-dimensional location of the emerging point of the ophthalmic artery. It can be located by one thumb finger -width above and 4mm medial to the medial canthus coordinate, respectively, in addition to a 5mm depth below the skin.

PART II: Arterial distribution of the forehead

For 17 cases (85 percent), an entire trunk of the sSTA were observed and emerged below the medial portion of the SOR, coursing upward along the frontalis lateral to the midline plane. The dSTA was located lateral to the Y axis (medial canthus plane) generally. For the two type Ia hemifaces, sSTA was broadly distributed to supply the frontalis. When the frontalis was excised and retracted, we found that the sSTA overlapped the dSTA and the dSOA (Fig. 17).

We found that the neurovascular bundles (dSOA and supraorbital nerve) emerged from the supraorbital foramen (or notch) at the lower margin of the orbital rim and ran through the periosteum with superolateral distribution. The dSOA pierced the frontalis at one to three sites; from these piercing points, the dSOA extended superficially to become the sSOA and to anastomose with the sSTA and the frontal branch of the superficial temporal artery and to supply the superolateral portion of the forehead.

The injection of dermal fillers into the forehead involves an assessment of forehead contour and a determination of the specific locations, depths, and volumes of filler to be injected. We maintain that the safety of filler injections can be improved with comprehensive knowledge of the arterial system of the forehead not only in the sagittal plane but also in the coronal plane.

Despite results from the current study, it was advocated that clinicians determine the entry and injection sites for dermal fillers according to three reference planes (Fig. 18): a horizontal plane located 20 mm above the supraorbital margin (i.e., the dSOA penetration plane), a vertical plane through the medial canthus, and a vertical plane through the supraorbital foramen. The supraorbital foramen can be identified by measuring one fingerbreadth (mean, 10.8±4.9 mm) laterally from the medial-canthus plane along the orbital rim. All of the reference planes are confined with the orbital rim inferiorly and lateral

canthus laterally. The needle should enter below the dSOA penetration plane (within 20 mm above the orbital rim) and lateral to the supraorbital foramen plane to avoid injury to superficial arterial branches and the neurovascular bundle associated with the SOA. Then, a 23- to 25-gauge cannula to avoid excessive pressure and vasculature puncture should be advanced gently along the plane above the periosteum medially. Finally, the injection should be made both medial to the medial-canthus plane to avoid the dSTA (which is frequently located laterally to it) and deep to the frontalis to avoid the sSTA and central artery or paracentral artery (which are located superficially to it). Slow retrograde injection technique is advised. If lateral augmentation is needed, manual molding from the medial injection site to the lateral area can be conducted. For a patient requiring only glabella augmentation, an entry point can be made on the metopion of the forehead because of its relatively unpronounced vessel dispersion. Because the supratrochlear and supraorbital nerves innervate the forehead, local anesthesia is required before filler injection to avoid unnecessary pain. After the injection, massaging the injected area and allowing the filler to spread throughout can prevent undulations on the surface.

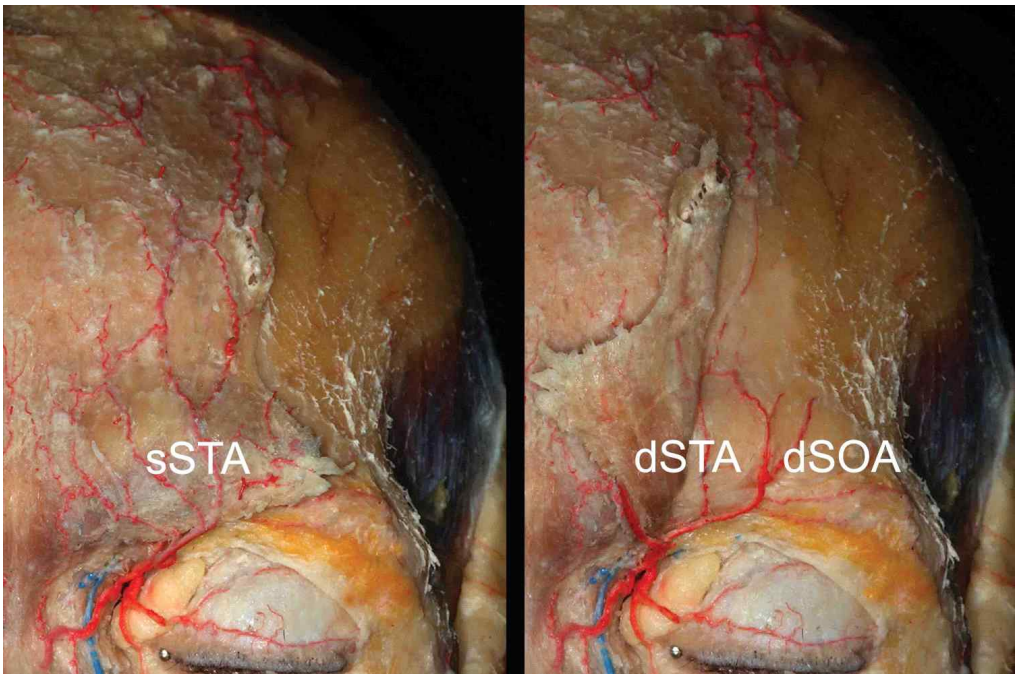

Figure 17. Overlapping cases of type Ia. Left panel: The superficial branch of supratrochlear artery (sSTA) was broadly distributed and supplied the frontalis; Right panel: Retraction of the frontalis revealed that the sSTA overlapped the deep branch of supratroclear artery (dSTA) and the deep branch of supraorbital artery (dSOA).

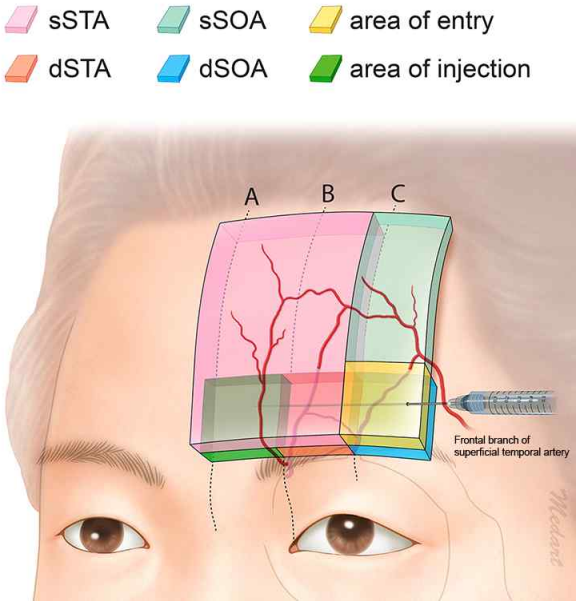

Figure 18. Guidelines for safe injection of dermal fillers into the forehead. Three reference planes should be considered within the confines of the orbital rim inferiorly and lateral canthus laterally: a horizontal plane 20 mm above the supraorbital margin [ie, the deep branch of supraorbital artery (dSOA) penetration plane], depicted as the uppermost margin of the yellow box; a vertical plane through the medial canthus (ie, the dotted line labeled B); and a vertical plane through the supraorbital foramen (SOF) (ie, the dotted line labeled C), which could be identified by palpation. The entry point (bounded by the yellow box) should be under the dSOA penetration plane and lateral to the SOF plane. The injection should be performed medially to the medial-canthus plane (dark green box) and deep to the frontalis. The superficial branch of supratrochlear artery (sSTA) and superficial branch of supraorbital artery (sSOA) are in dark red. The deep branch of supratrochlear artery (dSTA) and dSOA are in light red. A, midline plane; B, medial-canthus plane; C, SOF plane.

PART III: Anatomic location and courses of the inferior medial palpebral artery (IMPA)

The OA divides into the SMPA and IMPA, which supply the upper and lower eyelids, respectively (Erdogmus and Govsa, 2007). The structures constituting the medial eyelid include skin, subcutaneous tissue, the orbicularis oculi, the medial palpebral ligament, the orbital septum, septal fat, the tarsal plate, and conjunctiva. In this study, the OA, SMPA, and IMPA were located deep to the orbicularis oculi, with the OA positioned on septal fat as it emerged below the meidal portion of the SOR. The SMPA extended superiorly to the medial palpebral ligament and supplied the upper eyelid along the tarsal plate. After branching from the OA superior to the medial palpebral ligament, the IMPA extended inferolaterally to enter the lower eyelid nearly 4 mm lateral to the MC through a space (Fig. 13). Other authors have observed the IMPA to be located just behind the medial palpebral ligament before entering the lower eyelid (Erdogmus and Govsa, 2007 Edizer et al., 2009). We identified an inflection point of the IMPA in the lower eyelid, where it extended superolaterally from its initially inferolateral course. Thereafter, the inflection point that was 5 mm from the medial canthus transversely and 4 mm from the palpebral fissure vertically was the inferiormost position of the inferior medial palpebral artery in the lower eyelid. Finally, the IMPA communicated with the lateral palpebral artery of the lacrimal artery 2 mm inferior to the lateral canthus (type A extension) or penetrated the tarsal plate (type B extension). Of the 21 hemifaces with type A extension, nine hemifaces corresponded to type I distribution pattern, eight hemifaces were type II, and four hemifaces were type III. Of the nine hemifaces with type B extension, two hemifaces were type I, three hemifaces were type II, three hemifaces were type III, and one hemiface was type IV. It is known that the IMPA has a diameter of 1.0 mm and that the IMPA and SMPA may arise from the OA

jointly or individually before supplying the upper and lower eyelids. We found that the diameter of the IMPA in the lower eyelid was nearly 1 mm at the entry point and was 0.4 mm at the lateral canthus. Other authors have denoted the IMPA as a structure of the lower eyelid that lacked a detailed characterization (Kakizaki et al., 2009; Kakizaki et al., 2006). In this study, we examined the size, position, and distribution of the IMPA with respect to the SMPA and STA.

Tansatit et al. (2017) observed an embolic channel connecting the arterial system of the face to the OA. Li et al (2015) evaluated the previous reports of other authors to infer a likely pathway by which an injected filler droplet could access the OA. Following a temporal, frontal, or nasal injection, a filler droplet could enter the superficial temporal artery, STA, or dorsal nasal artery, respectively, by means of unintended puncture; this could lead to embolism in the OA and blindness.

Filler injection at the pretarsal roll poses a risk of vision loss caused by occlusion of the OA because the IMPA is vulnerable to damage during augmentation of the pretarsal roll. Filler injections at this site should be placed between the subcutaneous tissue and the pretarsal part of the orbicularis oculi in the lower eyelid. The courses of the IMPAs could be guessed, as they were located along the lower eyelashes and deep to the orbicularis oculi according to this study (Fig. 19). An injection that is too deep may result in an unpredictable and/or unfavorable shape of the pretarsal roll and may puncture the IMPA, which is located deep to the pretarsal part of the orbicularis oculi in the lower eyelid. An injection that is too shallow may result in the filler showing through the surface of the skin. The desired shape and volume of the pretarsal roll should be determined by observing the patient's smiling face. After treatment, the pretarsal roll should be slightly more pronounced, even when the patient is not smiling. The clinician should be careful to place filler

in a manner that preserves and enhances the patient's natural pretarsal roll. For instance, the pretarsal roll may grow wider from the lateral third of the eyelid or may be more pronounced at the lateral end.

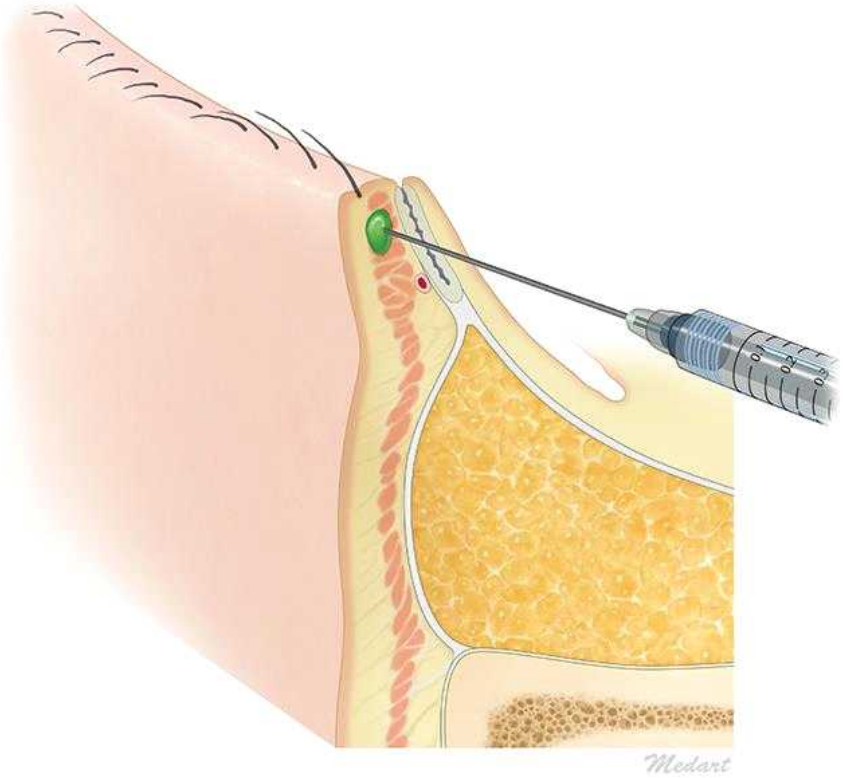

Figure 19. Appropriate injection (shown in green) into the pretarsal roll. Dermal fillers should be meticulously placed between the subcutaneous tissue and the pretarsal part of the orbicularis oculi.

Ⅴ. CONCLUSION

This study identified several Fbrs of OA including the location of EMP of OA, the distribution types of STA and SOA, and arterial courses of the IMPA. Importantly, these results and useful injection techniques provided for clinicians will contribute to safer outcomes when assessing the applications in the field of clinical interventions such as various dermal filler injections and UEMFs.

PART I: Three-dimensional (3D) identification of the emerging point of ophthalmic artery (EMP of OA)

Clinicians with detailed acknowledgement of the 3D location of the EMP of OA could avoid iatrogenic injury when performing minimally periorbital invasive and surgical procedures. Moreover, it is highly recommended that a US device be applied to preoperative examinations to help in identifying the location of the EMP of OA.

PART II: Arterial distribution of the forehead

Knowledge of vascular topography is essential to avoiding severe complications of filler injection into the forehead. The distributions of the STA and the SOA relative to the frontalis could be categorized into two main patterns. Our results emphasize the complexity of the forehead vasculature. We suggest a 3-plane reference system for determining the sites of needle entry and filler injection. Further study is warranted to validate the safety of these guidelines for forehead augmentation with dermal fillers.

PART III: Anatomic location and courses of the inferior medial palpebral artery (IMPA)

The results of this study indicate that the arterial branches of the upper and lower eyelids may be classified into four distributions and two extension types. All the IMPA located along the tarsal plate deep to the pretarsal part of the orbicularis oculi in the lower eyelid. The measurement of certain distance of the IMPA in the lower eyelid will help to identify the location of the artery.

REFERENCES

Arnuntasupakul V, Chalachewa T, Leurcharusmee P, et al: Ultrasound with neurostimulation compared with ultrasound guidance alone for lumbar plexus block: A randomised single blinded equivalence trial. Eur J Anaesthesiol. 2017.

Bass CB: Medial canthal ligament reconstruction. Ann Plast Surg 3:182-185, 1979.

Beer GM, Putz R, Mager K, Schumacher M, Keil W: Variations of the frontal exit of the supraorbital nerve: an anatomic study. Plast Reconstr Surg 102:334-341, 1998.

Bock A, Suschek CV, Oplander C, et al: Evaluation of facial blood flow using three-dimensional scanning. Br J Oral Maxillofac Surg 55:974-976, 2017.

Chang EI, Esmaeli B, Butler CE: Eyelid Reconstruction. Plast Reconstr Surg 140:724e-735e, 2017.

Chaves MTP, Martins-Costa S, Oppermann M, et al: Maternal ophthalmic artery Doppler ultrasonography in preeclampsia and pregnancy outcomes. Pregnancy Hypertens. 2017.

Cong LY, Lee SH, Tansatit T, Hu KS, Kim HJ: Topographic Anatomy of the Inferior Medial Palpebral Artery and Its Relevance to the Pretarsal Roll Augmentation. Plast Reconstr Surg 138:430e-436e, 2016.

Cong LY, Phothong W, Lee SH, et al: Topographic Analysis of the Supratrochlear Artery and the Supraorbital Artery: Implication for Improving the Safety of Forehead Augmentation. Plast Reconstr Surg 139:620e-627e, 2017.

Edizer M, Beden U, Icten N: Morphological parameters of the periorbital arterial arcades and potential clinical significance based on anatomical identification. J Craniofac Surg 20:209-214, 2009.

Erdogmus S, Govsa F: Anatomy of the supraorbital region and the evaluation of it for the reconstruction of facial defects. J Craniofac Surg 18:104-112, 2017.

Erdogmus S, Govsa F: The arterial anatomy of the eyelid: importance for reconstructive and aesthetic surgery. J Plast Reconstr Aesthet Surg 60:241-245, 2007.

Faris C, van der Eerden P, Vuyk H: The midline central artery forehead flap: a valid alternative to supratrochlear-based forehead flaps. JAMA Facial Plast Surg 17:16-22, 2015.

Frederic L: Potential use of the Upper Eyelid Myocutaneous Flap in the Reconstruction of Full-thickness Defects of the Medial Canthus. Surgery: Current Research 04, 2013.

Fukuta K, Potparic Z, Sugihara T, et al: A cadaver investigation of the blood supply of the galeal frontalis flap. Plast Reconstr Surg 94:794-800, 1994.

Han J, Kwon ST, Kim SW, Jeong EC: Medial and lateral canthal reconstruction with an orbicularis oculi myocutaneous island flap. Arch Plast Surg 42:40-45, 2015.

Hayreh SS: THE OPHTHALMIC ARTERY: III. BRANCHES. Br J Ophthalmol 46:212-247, 1962.

Kakizaki H, Chan WO, Takahashi Y, Selva D: Overriding of the preseptal orbicularis oculi muscle in Caucasian cadavers. Clin Ophthalmol 3:243-246, 2009.

Kakizaki H, Jinsong Z, Zako M, et al: Microscopic anatomy of Asian lower eyelids. Ophthal Plast Reconstr Surg 22:430-433, 2006

Kariya K, Usui Y, Higashi N, et al: Anatomical basis for simultaneous block of greater and third occipital nerves, with an ultrasound-guided technique. J Anesth. 2017.

Kim HJ, Seo KK, Lee HK, Kim J: Clinical Anatomy of the Face for Filler and Botulinum Toxin Injection: Springer Singapore. 2016.

Kim SW, Han HH, Jung SN: Orbicularis oculi myocutaneous island flap for upper eyelid reconstruction. J Craniofac Surg 23:746-748, 2012.

Kim YS, Choi DY, Gil YC, et al: The anatomical origin and course of the angular artery regarding its clinical implications. Dermatol Surg 40:1070-1076, 2014.

Kleintjes WG: Forehead anatomy: arterial variations and venous link of the midline forehead flap. J Plast Reconstr Aesthet Surg 60:593-606, 2007.

Lee KW, Kim SH, Gil YC, Hu KS, Kim HJ: Validity and reliability of a structured-light 3D scanner and an ultrasound imaging system for measurements of facial skin thickness. Clin Anat 30:878-886, 2017.

Li X, Du L, Lu JJ: A Novel Hypothesis of Visual Loss Secondary to Cosmetic Facial Filler Injection. Ann Plast Surg 75:258-260, 2015.

Maruyama S: A Histopathologic Diagnosis of Vascular Occlusion After Injection of Hyaluronic Acid Filler: Findings of Intravascular Foreign Body and Skin Necrosis. Aesthet Surg J 37:NP102-NP108, 2017.

Rho NK, Park JY, Youn CS, Lee SK, Kim HS: Early Changes in Facial Profile Following Structured Filler Rhinoplasty: An Anthropometric Analysis Using a 3-Dimensional Imaging System. Dermatol Surg 43:255-263, 2017.

Robinson TJ, Stranc MF: The anatomy of the medial canthal ligament. Journal of Plastic, Reconstructive & Aesthetic Surgery 23:1-7, 1970.

Seyhan T: The figure-of-eight radix nasi flap for medial canthal defects. J Craniomaxillofac Surg 38:455-459, 2013.

Shin KJ, Shin HJ, Lee SH, et al: Emerging Points of the Supraorbital and Supratrochlear Nerves in the Supraorbital Margin With Reference to the Lacrimal Caruncle: Implications for Regional Nerve Block in Upper Eyelid

and Dermatologic Surgery. Dermatol Surg 42:992-998, 2016.

Skaria AM: The median forehead flap reviewed: a histologic study on vascular anatomy. Eur Arch Otorhinolaryngo 272:1231-1237, 2015.

Standring S: Gray's Anatomy 40th Edition. 2008.

Tansatit T, Apinuntrum P, Phetudom T: Facing the Worst Risk: Confronting the Dorsal Nasal Artery, Implication for Non-surgical Procedures of Nasal Augmentation. Aesthetic Plast Surg 41:191-198, 2017.

Tirone L, Schonauer F, Sposato G, Molea G: Reconstruction of lower eyelid and periorbital district: an orbicularis oculi myocutaneous flap. J Plast Reconstr Aesthet Surg 62:1384-1388, 2009.

Ugur MB, Savranlar A, Uzun L, Kucuker H, Cinar F: A reliable surface landmark for localizing supratrochlear artery: medial canthus. Otolaryngol Head Neck Surg 138:162-165, 2008.

Vural E, Batay F, Key JM: Glabellar frown lines as a reliable landmark for the supratrochlear artery. Otolaryngol Head Neck Surg 123:543-546, 2000.

Woo SW, Lee HJ, Nahm FS, Lee PB, Choi EJ: Anatomic characteristics of supraorbital foramina in korean using three-dimensional model. Korean J Pain 26:130-134, 2013.

Wu S, Pan L, Wu H, et al: Anatomic Study of Ophthalmic Artery Embolism Following Cosmetic Injection. J Craniofac Surg 28:1578-1581, 2017.

Yang HM, Kim HJ: Anatomical study of the corrugator supercilii muscle and its clinical implication with botulinum toxin A injection. Surg Radiol Anat 35:817-821, 2013.

Yoshioka N, Rhoton AL, Jr: Vascular anatomy of the anteriorly based pericranial flap. Neurosurgery 57:11-16; discussion 11-16, 2005.

Yu D, Weng R, Wang H, Mu X, Li Q: Anatomical study of forehead flap with its pedicle based on cutaneous branch of supratrochlear artery and its application in nasal reconstruction. Ann Plast Surg 65:183-187, 2010.

Zhao YJ, Xiong YX, Wang Y: Three-Dimensional Accuracy of Facial Scan for Facial Deformities in Clinics: A New Evaluation Method for Facial Scanner Accuracy. PLoS One 12:e0169402, 2017.

Zheng Y, Zhou Y, Zhou H, Gong X: Ultrasound image edge detection based on a novel multiplicative gradient and Canny operator. Ultrason Imaging 37:238-250, 2015.

Abstract (in korean)

눈동맥 출현점 및 눈동맥 얼굴가지의 국소해부학

<지도교수 김 희 진>

연세대학교 대학원 치의학과

총여요

얼굴에 분포하는 눈동맥의 주요 가지는 하나의 큰 줄기로 눈확의 앞쪽으로 빠져나와 큰 동맥 연결을 형성하여, 이마 (도르래위동맥, STA), 코 (콧등동맥, DNA), 안쪽눈구석 (눈구석동맥, AA)과 눈꺼풀 (위 및 아래안쪽눈꺼풀동맥, SMPA and IMPA) 부위에 분포한다.

임상적으로는 비침습적인 필러 시술과 재건 수술과 관련한 위눈꺼풀근육피부피판 (upper eyelid myocutaneous flap (UEMF)) 술식 등에 눈동맥의 출현점 및 가지들에 대한 임상해부학적 지식이 필수적이다. 필러 시술은 일반적으로 임상에서 얼굴 미용 시술로 널리 이용되고 있으며, 시술시 눈동맥의 얼굴가지에 대한 해부학적 지식의 부재는 동맥의 손상을 일으켜 동맥 분포부위의 피부 괴사 등, 극히 드물게는 실명도 초래할 수 있다. 또한 위눈꺼풀근육피부피판 (upper eyelid myocutaneous flap (UEMF))은 눈주위 조직 재건에 적용되는 눈성형술로, UEMF 시 눈동맥의 출현점 및 동맥가지에 대한 해부학적 지식은 성공적인 피판수술을 위해 중요하다. 따라서 본 연구에서는 위와 같은 동맥들이 일어나는 동맥의 줄기 부분을 눈동맥의 얼굴가지 (Fbrs of OA)로 명명하여 그 출현점과 분포양상을 관찰하였다.

본 연구의 목적은 (1) 얼굴에서 눈동맥이 나타나는 동맥 출현점의 3차원적 구명, (2) 이마부위에 분포하는 도르래위동맥 (STA)과 눈확위동맥 (SOA)의 분포양상 관찰, (3) 아래안쪽눈꺼풀동맥의 국소해부학적 분석을 통해 안전한 눈주위 최소침습적 치료 및 수술적 치료에 기여할 수 있는 임상적 가이드라인을 제시하는

것이다.

재료로는 17쪽의 시신을 3D 스캐너 (Morpheus3D®, Morpheus Company, Seongnam, Korea)를 이용하여 정면과 양쪽 45° 측면에서 얼굴을 촬영하였다. 촬영한 얼굴은 Morpheus Plastic Solution (version 3.0) 프로그램을 이용하여 정면과 양쪽 측면에서 촬영해 획득한 세 개의 사진을 세 점 (가쪽눈구석, 콧방울점, 입꼬리)을 기준으로 정합하여 3차원 재구성하였다. 오른쪽 안쪽눈구석을 지나는 수직선을 따라 절개선을 긋고 피부를 벗겨 해부를 진행하였다. 눈동맥 출현점을 노출한 후 처음과 같은 방법으로 해부가 된 시신의 얼굴을 3D 스캐너를 이용하여 촬영하였다. 해부가 되지 않은 사진과 눈동맥 출현점 해부가 된 사진을 최종적으로 정합하여 3차원 이미지를 획득하였다. 이와 함께, 30명의 임상시험 피험자를 대상으로 초음파 촬영하여 눈동맥 출현점을 관찰하였다. 더불어 20쪽의 시신을 해부하여 이마 부위의 혈관분포 양상을 관찰하였으며 31쪽의 시신을 이용하여 아래안쪽눈꺼풀동맥을 조사하였다.

본 연구를 통해 얻은 결과는 다음과 같다.

눈동맥의 3차원적 출현점은 안쪽눈구석에서 안쪽으로 3.8±1.0 mm, 위쪽으로 14.0±2.9 mm 떨어진 곳에 위치하였다. 3D 스캐너 및 초음파를 이용하여 계측한 피부에서부터 눈동맥 출현점의 깊이는 각각 4.8±1.7 mm, 4.5±1.1 mm였다.

이마에 분포하는 도르래위동맥 깊은가지의 유무에 따라 두 개의 주요 동맥 분포양상이 관찰되었다. Type I (도르래위동맥의 깊은가지 (dSTA)가 존재하는 경우, 55%)은 두 개의 세부 형태로 나누었다. Type Ia (35%)는 이마근 얕은층의 안쪽부분은 도르래위동맥의 얕은가지 (sSTA)가 분포하고 가쪽부분은 눈확위동맥의 얕은가지 (sSOA)가 분포하는 형태였다. 또한 도르래위 및 눈확위동맥의 깊은가지가 이마근의 깊은 부분에 분포하였다. Type Ib (20%)는 이마근의 얕은층의 안쪽은 도르래위동맥의 얕은가지와 중심동맥 (central artery) 혹은 중심옆동맥 (paracentral artery)이 분포하며 가쪽은 눈확위동맥의 얕은가지가 분포하는 형태였다. 또한 이 유형에서 도르래위 및 눈확위동맥의 깊은가지가 이마근의 깊은부분에 분포하였다. Type II (도르래위동맥의 깊은가지 (dSTA가 부재한 경우, 45%)는 이마근의 얕은부분은 도르래위동맥의 얕은가지가 가쪽부분은 눈확위동맥의 얕은

가지가 분포하였으며 눈확위동맥의 깊은가지가 이마근의 깊은부분에 모두 분포하는 형태로 관찰되었다.

아래안쪽눈꺼풀동맥의 분포양상은 네 가지 형태로 관찰되었다. Type I은 위 및 아래안쪽눈꺼풀동맥이 눈동맥에서 각각 독립적으로 분지하고 눈동맥은 도르래위동맥으로 계속되며 끝나는 형태로 36.7%에서 관찰되었다. Type II는 눈동맥에서 짧은 하나의 가지가 분지되고 이 가지에서 위 및 아래안쪽눈꺼풀동맥이 나뉘고 눈동맥은 도르래위동맥으로 계속되어 끝나는 형태로 36.7%에서 관찰되었다. Type III는 위 및 아래안쪽눈꺼풀동맥이 눈동맥 한 지점에서 일어나고, 눈동맥은 도르래위동맥으로 끝나는 형태로 23.3%에서 관찰되었다. Type IV는 위 및 아래안쪽눈꺼풀동맥이 눈동맥의 끝가지에서 분지하고, 도르래위동맥은 눈구석동맥에서 오는 형태로 3.3%에서 관찰되었다.

본 연구에서 관찰된 결과를 적용하여 다양한 필러 시술과 UEMF 수술을 진행한다면 효과적인 수술 결과를 얻을 수 있을 것으로 생각한다.

핵심 되는 말 : 눈동맥 출현점; 도르래위동맥, 눈확위동맥, 아래안쪽눈꺼풀동맥, filler augmentation; 3D 스캐너; 초음파 영상 장비